Translational Oncology 13 (2020) 100831

Contents lists available at ScienceDirect

Translational Oncology

journal homepage: www.elsevier.com/locate/tranon

Multiparametric MRI-based radiomics analysis for the prediction of breast tumor regression patterns after neoadjuvant chemotherapy

Xiaosheng Zhuang [a,b,1], Chi Chen [c,d,1], Zhenyu Liu [d,e], Liulu Zhang [a], Xuezhi Zhou [d,f], Minyi Cheng [a], Fei Ji [a], Teng Zhu [a], Chuqian Lei [a,g], Junsheng Zhang [a,b], Jingying Jiang [h,i,*], Jie Tian [d,e,f,h,i,**], Kun Wang [a,***]

[a] Department of Breast Cancer, Cancer Center, Guangdong Provincial People's Hospital, Guangdong Academy of Medical Sciences, Guangzhou 510080, China
[b] Shantou University Medical College, Shantou 515041, Guangdong, China
[c] School of Biological Science and Medical Engineering, Beihang University, Beijing 100191, China
[d] Key Laboratory of Molecular Imaging, Institute of Automation, Chinese Academy of Sciences, Beijing 100190, China
[e] School of Artificial Intelligence, University of Chinese Academy of Science, Beijing 100080, China
[f] Engineering Research Center of Molecular and Neuro Imaging of Ministry of Education, School of Life Science and Technology, Xidian University, Xi'an, Shaanxi 710126, China
[g] The Second School of Clinical Medicine, Southern Medical University, Guangzhou 510515, China
[h] Beijing Advanced Innovation Center for Big Data-Based Precision Medicine, School of Medicine and Engineering, Beihang University, Beijing 100191, China
[i] Key Laboratory of Big Data-Based Precision Medicine (Beihang University), Ministry of Industry and Information Technology, Beijing 100191, China

ARTICLE INFO

Article history:
Received 3 May 2020
Received in revised form 8 June 2020
Accepted 11 June 2020
Available online xxxx

ABSTRACT

Objectives: Breast cancers show different regression patterns after neoadjuvant chemotherapy. Certain regression patterns are associated with more reliable margins in breast-conserving surgery. Our study aims to establish a nomogram based on radiomic features and clinicopathological factors to predict regression patterns in breast cancer patients.
Methods: We retrospectively reviewed 144 breast cancer patients who received neoadjuvant chemotherapy and underwent definitive surgery in our center from January 2016 to December 2019. Tumor regression patterns were categorized as type 1 (concentric regression + pCR) and type 2 (multifocal residues + SD + PD) based on pathological results. We extracted 1158 multidimensional features from 2 sequences of MRI images. After feature selection, machine learning was applied to construct a radiomic signature. Clinical characteristics were selected by backward stepwise selection. The combined prediction model was built based on both the radiomic signature and clinical factors. The predictive performance of the combined prediction model was evaluated.
Results: Two radiomic features were selected for constructing the radiomic signature. Combined with two significant clinical characteristics, the combined prediction model showed excellent prediction performance, with an area under the receiver operating characteristic curve of 0.902 (95% confidence interval 0.8343–0.9701) in the primary cohort and 0.826 (95% confidence interval 0.6774–0.9753) in the validation cohort.
Conclusions: Our study established a unique model combining a radiomic signature and clinicopathological factors to predict tumor regression patterns prior to the initiation of NAC. The early prediction of type 2 regression offers the opportunity to modify preoperative treatments or aids in determining surgical options.

Introduction

Preoperative neoadjuvant chemotherapy (NAC) has played an increasingly significant role in comprehensive care for locally advanced breast cancers [1]. The primary purposes of NAC are to downstage breast cancers and improve the possibility of breast-conserving therapy in most breast cancers [2–4]. After preoperative chemotherapy, breast tumors shrink to different extents and show various regression patterns, including pathologic complete response (pCR), unifocal shrinkage, multiple residual foci, main residual disease with satellite foci, stable disease (SD) and progressive disease (PD) [5–8]. Among these patterns, unifocal residual disease and pCR favor the adoption of breast-conserving surgery (BCS). Patients with

Abbreviations: BCS, breast-conserving surgery; ER, estrogen receptor; HER-2, human epidermal growth factor receptor 2; NAC, neoadjuvant chemotherapy; PC, primary cohort; pCR, pathologic complete response; PD, progressive disease; PR, progesterone receptor; SD, stable disease; VC, validation cohort.

* Correspondence to: J. Jiang, Beijing Advanced Innovation Center for Big Data-Based Precision Medicine, School of Medicine and Engineering, Beihang University, Beijing, 100191, China.
** Correspondence to: J. Tian, Institute of Automation, Chinese Academy of Sciences, No. 95 Zhongguancun East Road, Haidian District, Beijing 100190, China.
*** Correspondence to: K. Wang, Department of Breast Cancer, Cancer Center, Guangdong Provincial People's Hospital, Guangdong Academy of Medical Sciences, 106, Zhongshan ER Lu, Guangzhou 510080, China.
E-mail addresses: jingyingjiang@buaa.edu.cn, (J. Jiang), jie.tian@ia.ac.cn, (J. Tian), gzwangkun@126.com. (K. Wang).
[1] Xiaosheng Zhuang and Chi Chen contributed equally to this work.

http://dx.doi.org/10.1016/j.tranon.2020.100831

multiple residual foci, SD and PD are, however, more prone to undergoing mastectomy after completing NAC.

The higher local recurrence rate in NAC than in adjuvant chemotherapy has caused breast cancer specialists to take caution. In a recent meta-analysis, the 15-year local recurrence rate in patients receiving NAC was found to be 5.5% higher than that in patients receiving chemotherapy (21.4% vs 15.9%, $p = 0.0001$) [9]. An increase in the BCS rate was speculated to be responsible for this finding since patients with favorable responses to NAC may have successfully changed their original intended surgical plan from mastectomy to BCS. Though the higher IBTR did not cause a significant difference in overall survival, it brought an extra operation and might cause mental stress to patients. A previous study from the University of Pittsburgh determined that multifocal regression independently predicts IBTR [6]. Tumor regression patterns were divided into 2 types: pCR plus unifocal regression and multifocal regression. Compared to that in the pCR group, the hazard ratio of tumor recurrence reached 11.2 in the diffuse multifocal regression group. Meanwhile, 9.5% of the patients were recruited for a second operation as a result of the positive margins in their first attempted breast-conserving surgery.

Because satellite/microfoci remain after neoadjuvant chemotherapy, the negative margins in BCS may not be as safe in cancers with multifocal regression. In patients with poor response to NAC, including PD and SD, BCS is obviously not a preferred option. Nakamura [10] categorized tumor regression patterns into concentric regression and dendritic regression and determined that nonconcentric regression necessitated careful evaluation for BCS. In this study, tumor regression patterns are categorized into 2 types based on clinical interest. Type 1 regression contains pCR and unifocal regression, for which BCS is the more favored surgical plan. Type 2 regression is composed of multiple residual foci, main residual disease with satellite foci, stable disease (SD) and progressive disease (PD), which are appropriate candidates for mastectomy. In addition to patients' willingness and contraindications to radiation therapy [11], the tumor regression pattern is crucial for determining whether BCS is feasible for an individual patient. Accordingly, the early prediction of the tumor regression pattern is of great value and needs to be studied. The baseline prediction of tumor regression patterns identifies BCS candidates at an early phase. This enables the early modification of treatment strategies for those predicted to have a type 2 regression with great possibility after NAC. In specific molecular subtypes, e.g., TNBC, a more vigorous platinum-based chemotherapy may be adopted in non-BCS candidates to obtain a better chemotherapy response [12].

Radiomics has become a novel tool for noninvasively obtaining anatomical tumor information by extracting and analyzing quantitative imaging features [13]. Dedicated MRI imaging assists oncologists in providing higher quality medical services, including more precise diagnoses [14,15], improved predictions of lymph node metastasis [16] and more accurate treatment response assessments [17,18]. Previously, Liu [19] and Xiong [20] explored the possibility of multiparametric MRI in predicting the treatment response after NAC, focusing on pCR or Miller–Payne grade. Few studies have concentrated on predicting tumor regression patterns that are closely related to surgical options. In this original article, we tried to reveal the correlations between a radiomic signature plus clinicopathological factors and tumor regression patterns.

Material and methods

Patients and factors

We retrospectively enrolled 144 patients with stage II-III breast cancers who received NAC and underwent surgery in Guangdong Provincial People's Hospital between February 2016 and June 2019. The criteria for patient inclusion were as follows: 1) biopsy-confirmed invasive breast cancer with no distant metastatic disease; 2) no missing baseline clinicopathological factors; 3) MRI examinations in our center prior to biopsy; and 4) definitive surgery following standard preoperative chemotherapy. The exclusion criteria were as follows: 1) missing baseline characteristics; 2) no available MR images or only poor-quality images; 3) patients underwent final surgery at another cancer center and pathologic results were unavailable; and 4) patients did not complete the planned cycles of NAC regimen or had nonstandard NAC treatment (e.g., trastuzumab was not included in the presurgical chemotherapy). We randomly allocated 7/10 of eligible patients to primary cohort and the remaining to validation cohort in a 7:3 ratio.

In this retrospective study, each enrolled patient underwent the planned standard chemotherapy regimen as recommended by the NCCN Breast Cancer Guidelines. The preoperative chemotherapy regimens suggested by qualified oncologists were taxane-based, anthracycline-based or a combination of the two. Furthermore, for patients with HER-2 positive status, anti-HER-2 therapy (e.g., trastuzumab) was added in the treatment. This study was approved by the Ethics Committee of Guangdong Provincial People's Hospital. The requirement for informed consent was waived with authorization because our study had a retrospective design and did not involve any additional interventions.

Immunohistochemistry (IHC)

IHC was performed for each patient to determine the baseline estrogen receptor (ER) status, progesterone receptor (PR) status, HER-2 status, and Ki67 status. The cutoff value for ER and PR was set at 1% [21], and the cutoff value for Ki67 was 20% [22,23]. In regard to HER-2 status, tumors with an IHC staining of 0 to 1+ were defined as HER-2 negative and 3+ as HER-2 positive. For tumors with an IHC score of 2+, ISH testing was further performed to confirm the HER-2 status. A non-amplified ISH result denotes the HER-2 status as negative, and an amplified result denotes the HER-2 status as positive.

Determination of tumor regression patterns

The tumor regression patterns were determined based on the final surgical specimen. The patients underwent either BCS or mastectomy after completing NAC. In either surgical procedure, the operation zone covered the area of the primary cancer. Standard pathologic analyses were performed for the assessment of the residual tumor after preoperative chemotherapy. The surgical specimens were fixed with standard formalin solution by experienced breast pathologists and processed in standard breast tissue processors, after which the specimens were cut in parallel in a continuous manner to expose the cancer tissue. For each slice, a 5 mm slide was further prepared for H&E staining. The longest diameter of the residual invasive tumor was recorded. Type 1 regression included pCR and unifocal regression. The former was defined as no residual invasive cancer remaining after NAC (ypTis allowed). The latter was designated unifocal residual cancer tissue when the area of the original cancer with the longest diameter shrank at least 30%. Type 2 regression comprised multiple residual foci, main residual disease with satellite foci, stable disease (SD) and progressive disease (PD). Multiple residual foci showed at least 2 separate foci in the continuous slides, whereas main residual disease with satellite foci showed a dominant residual disease with at least 1 minor accompanying focus. SD and PD were defined according to RECIST version 1.1 [24]. PD indicated an increase of $\geq 20\%$ in the largest diameter of the tumor. SD indicated an increase of less than 20% or a decrease of less than 30% in the tumor's largest diameter (Fig. 1). Three breast pathologists with more than 15 years of experience interpreting breast specimens independently examined the specimens and determined the tumor regression pattern based on the H&E-stained slides. Agreements were made on the tumor regression patterns among the 3 pathologists to reduce possible errors caused by interobserver variability.

ROI masking and radiomic feature extraction

The patients underwent breast MRI examination within one week prior to the biopsy using a field strength magnet of 1.5 T or 3.0 T. Two imaging sequences, including diffusion-weighted imaging (DWI) and fat-suppressed

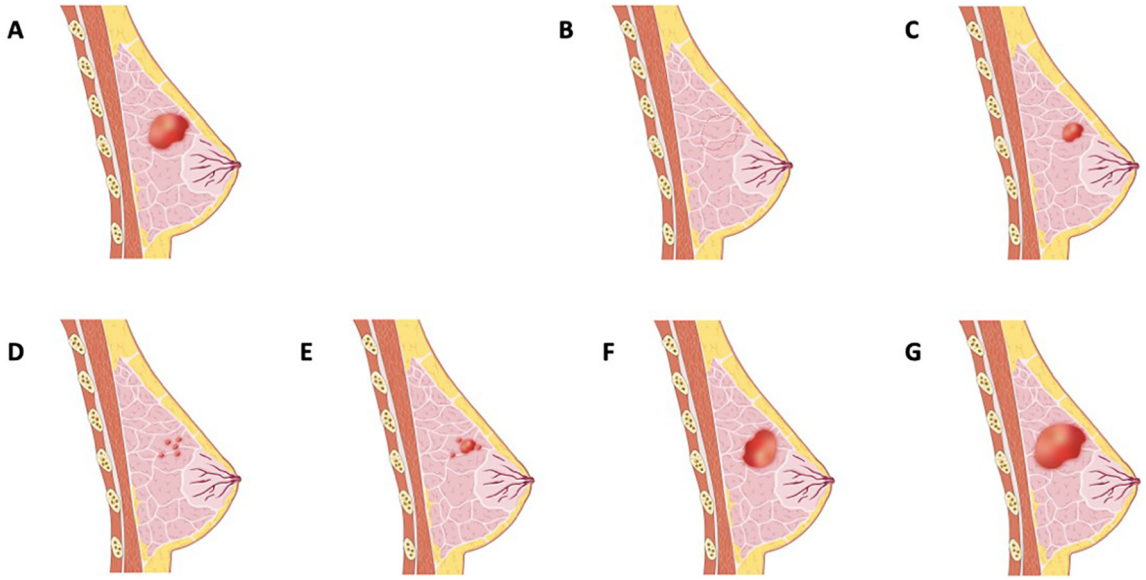

Fig. 1. Tumor regression patterns after neoadjuvant chemotherapy. a Primary cancer. b Type 1 regression (complete remission). c Type 1 regression (concentric regression). d Type 2 regression (multiple residual foci). e Type 2 regression (a main residual disease with satellite foci). f Type 2 regression (stable disease). g Type 2 regression (progressive disease).

T2-weighted imaging (T2WI), were acquired for each patient. T2WIs were obtained before the injection of contrast, and DWI sequences were collected at 2 b values (b = 0 and 1000 s/mm2) after the completion of dynamic contrast-enhanced imaging.

Two radiologists with 10 years of experience were responsible for tumor masking. For each MRI series, they evaluated the boundary of the tumor independently. For any disagreements, a third consulting radiologist with at least 30 years of experience determined the tumor border through discussion to decrease the interobserver variability. Tumor contours on every slice in DCE were manually delineated using ITK-SNAP (www.itksnap.org), excluding vessels and hemorrhagic or necrotic foci. With the help of the calibration tool and wipe tool in ITK-SNAP, the acute masking of ROI in T2WI and DWI was assured (Fig. 2).

By applying the feature extractor function of the "radiomics" package in Python (version: 3.7; www.python.org), each sequence of the MR images had 1158 multidimensional features extracted.

Feature screening and radiomic signature construction

First, we performed Mann-Whitney *U* test screening on T2WI and ADC sequence features, retaining features with *p* values less than 0.05. Then, the elastic network chose the residual features (11 from T2WI; 229 from ADC), and the predictive features were selected. Model convergence was achieved through a five-fold cross-validation strategy. The support vector machine (SVM) is a nonlinear classifier with a radial basis function kernel. The SVM was trained based on features from PC and determined parameters by the five-fold cross-validation strategy. The radiomic signature was computed for each patient in the validation cohort via the SVM model, and ROC curves and areas under the ROC curve (AUCs) were calculated.

Feature selection was implemented by the 'radiomics' package of Python (version: 3.7; www.python.org), and radiomic signature construction was implemented by the 'sklearn' package of Python (version: 3.7; www.python.org).

Construction of the clinical and combined models

The commonly used clinicopathological factors, including age, node stage, tumor stage, PR status, ER status, and neoadjuvant chemotherapy (NAC) regimen, were prepared for building a clinical prediction model. Significant characteristics were selected using backward stepwise selection, after which these filtered indicators were used to construct a clinical prediction model applying multivariate logistic regression.

Regarding the construction of the final model, based on the screened clinicopathological factors and the radiomic signature, a multivariate logistic regression model was constructed.

The ROC curves and AUC values of the clinical model and combination model were calculated to assess the predictive ability of the models.

Both the clinical and combined model were implemented by R software (version 3.6.2; http://www.Rproject.org) with the package 'glm2'.

Evaluations of the prediction models' performance

ROC curve analysis is often used to assess the predictive performance of radiomic signatures and clinical and combined models. The ROC analysis was implemented through the 'pROC' package in R software (version 3.6.2; http://www.Rproject.org). To further compare the performance measures of the prediction models, we employed decision curve analysis (DCA) in both the primary and validation cohort. Furthermore, the net reclassification index (NRI) and the integrated discrimination improvement (IDI) between the two different models were also calculated to evaluate their performance. Finally, we presented the most predictive model as a nomogram and calibration curve analysis was employed to evaluate the nomogram.

Results

Clinical characteristics

A total of 144 patients were recruited into the study, with a median age of 49 years (range 24–73 years). Clinical features of 144 patients and their associations with regression patterns are shown in Table 1. One hundred patients were included in the primary cohort (PC), and 44 were included in the validation cohort (VC). There was no significant difference in the proportion of type 2 shrinkage (17% and 18% in the PC and VC, respectively, $p = 1$) in the two cohorts and no significant difference in the type 2 shrinkage ratio of different molecular types (luminal of 20.8%, HER2 positive of 12.0%, TNBC of 8.7%, $p = 0.327$) in the cohorts.

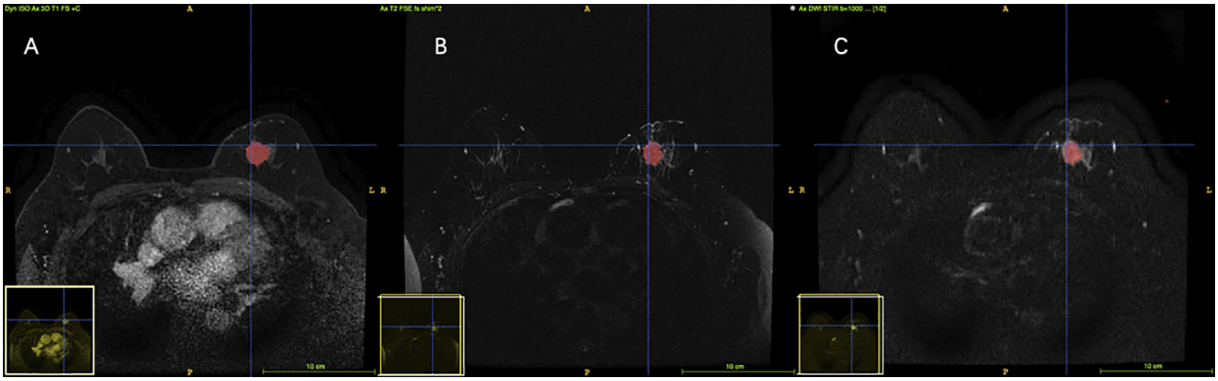

Fig. 2. Tumor masking in different MR sequences. a. DCE b. T2WI c. DWI.

Feature selection and radiomic signature construction

Two salient features (Original_shape_Sphericity and Log-sigma-3-0-mm-3D_firstorder_MeanAbsoluteDeviation) from T2WI and ADC, respectively, were finally selected through the Mann-Whitney *U* test and elastic network to prepare for the construction of a radiomic signature.

Construction of the clinical and combined models

Two significant clinicopathological indicators, namely, node stage and ER status, were selected through backward stepwise selection, after which they were incorporated into building a clinical prediction model. The selected clinical indicators and the radiomic signature were utilized to create a combined model. The relevant parameters of the clinical model and the combined prediction model are listed in Tables 2 and 3, respectively.

Evaluations of the prediction models' performance

In the ROC analysis, the area under the ROC curve (AUC) of the radiomic signature has reached 0.858 (95% CI: 0.7762–0.9389) in the PC and 0.819 (95% CI: 0.619–1) in the VC. The clinical prediction model yielded an AUC of 0.709 (95% CI: 0.5942–0.8239) in the PC and 0.597 (95% CI: 0.3122–0.8823) in the VC. Regarding the combined model, it achieved a performance with an AUC of 0.902 (95% CI: 0.8343–0.9701) in the PC and 0.826 (95% CI: 0.6774–0.9753) in the VC (Fig. 3). In the ROC curve analysis of the clinical and combined model, the AUC was increased by 0.193 in the PV and by 0.229 in the VC. This result shows that the predictive ability of the combined prediction model was significantly improved in both cohorts.

Table 1
Clinical features of 144 patients and their associations with regression patterns.

Factors	Primary cohort		P value	Validation cohort		P value
	Type 1 regression	Type 2 regression		Type 1 regression	Type 2 regression	
Age (years), mean ± SD	50.24 ± 9.33	47.82 ± 8.89	0.344	48.50 ± 9.32	49.25 ± 13.56	0.709
Menopausal status			0.877			0.524
Premenopausal	59 (71.1%)	13 (76.5%)		25 (69.4%)	4 (50.0%)	
Postmenopausal	24 (28.9%)	4 (23.5%)		11 (30.6%)	4 (50.0%)	
ER status			0.014			0.652
≤1%	36 (43.4%)	2 (11.8%)		8 (22.2%)	3 (37.5%)	
>1%	47 (56.6%)	15 (88.2%)		28 (77.8%)	5 (62.5%)	
PR status			0.090			0.423
≤1%	38 (45.8%)	4 (23.5%)		10 (27.8%)	4 (50.0%)	
>1%	45 (54.2%)	13 (76.5%)		26 (72.2%)	4 (50.0%)	
HER2 status			0.797			0.695
Positive	37 (44.6%)	7 (41.2%)		11 (30.6%)	3 (37.5%)	
Negative	46 (55.4%)	10 (58.8%)		25 (69.4%)	5 (62.5%)	
Ki67 status			0.258			1
≤20%	16(19.3%)	6(35.3%)		12(33.3%)	3(37.5%)	
>20%	67(80.7%)	11(64.7%)		24(66.7%)	5(62.5%)	
T stage			0.390			0.080
T2	73 (88.0%)	13 (76.5%)		35 (97.2%)	6 (75.0%)	
T3–4	10 (12.0%)	4 (23.5%)		1 (2.8%)	2 (25.0%)	
N stage			0.304			0.053
0	49 (59.1%)	7 (41.2%)		20 (55.5%)	1 (12.5%)	
1	29 (34.9%)	7 (41.2%)		12 (33.3%)	4 (50.0%)	
2	4 (4.8%)	2 (11.7%)		2 (5.6%)	3 (37.5%)	
3	1 (1.2%)	1 (5.9%)		2 (5.6%)	0 (0.0%)	
Molecular subtype			0.050			0.464
Luminal	47 (56.6%)	15 (88.2%)		29 (80.6%)	5 (62.5%)	
HER2 over-expressed	19 (22.9%)	1 (5.9%)		3 (8.3%)	2 (25.0%)	
TNBC	17 (20.5%)	1 (5.9%)		4 (11.1%)	1 (12.5%)	
NAC regimen			1.000			0.710
Anthracycline based	22 (26.5%)	4 (23.5%)		15 (41.7%)	4 (50.0%)	
Non-anthracycline based	61 (73.5%)	13 (76.5%)		21 (58.3%)	4 (50.0%)	

ER estrogen receptor, *PR* progesterone receptor, *HER2* human epidermal growth factor receptor 2, *NAC* neoadjuvant chemotherapy.

Table 2
Details of the clinical prediction model.

Intercept and variable	Clinical prediction model		
	Coefficient	Odds ratio (95% CI)	*p*
Intercept	3.5430087	–	3.55e-05
N stage	−0.7868074	0.45530 (0.210980– 0.982540)	0.0450
ER status	−1.9374503	0.14407 (0.028898– 0.718270)	0.0181

ER estrogen receptor.

Table 3
Details of the combined prediction model.

Intercept and variable	Combined prediction model		
	Coefficient	Odds ratio (95% CI)	*p*
Intercept	4.2903	–	0.0003
Radiomic signature	1.7605	19.43400 (4.247300– 88.92700)	0.0001
N stage	−1.3315	0.26408 (0.086122– 0.80978)	0.0199
ER status	−2.1500	0.11648 (0.016337– 0.83049)	0.0319

ER estrogen receptor.

The decision curve of the three prediction models showed that the combined model could achieve the maximum net benefit, as shown in Fig. 4. We took the combined prediction model as the new model, the clinical prediction model and the radiomic signature as the old model, respectively. The NRI and IDI were 0.3877 ($p = 0.0013$) and 0.2692 ($p < 0.001$), respectively, between the clinical model and the combined model. The NRI and the IDI between the signature and the combined model were calculated to be 0.3529 ($p = 0.00287$) and 0.1212 ($p = 0.00887$), respectively. As can be seen from the values of NRI and IDI, the new model (the combined prediction model) had improved prediction performance compared to the old model (the clinical prediction model; the radiomic signature). Therefore, the combined model is the most predictive for type 1 regression. A nomogram consisting of node stage, ER status, and the radiomic signature was created and its calibration curve illustrated good concordance between the predicted and actual outcomes of type 1 regression, as shown in Fig. 5.

Discussion

In this study, we studied the correlations between tumor regression patterns and MRI characteristics. A model combining the multiparametric MRI signature, node stage and ER status was established to predict tumor regression patterns after NAC at a very early stage. The model achieved an AUC of 0.902 in the PC and 0.826 in the VC.

Breast-conserving surgery is one of the purposes of receiving NAC. It has been clearly indicated that a clear surgical margin is the key to the success of BCS. In clinical practice, however, the recurrence rate is somewhat higher in patients receiving NAC than in those receiving chemotherapy, which can be explained by false negative margins in surgery. Ling et al. divided tumor regression patterns into 2 categories [6]. Patients with pCR and unifocal residual disease after NAC had a higher rate of 4-year IBTR-free survival than those with multifocal disease. Based on clinical interest, we categorized tumor regression patterns into 2 types as well. Patients with type 2 regression show an inadequate response to the planned preoperative therapy, with either satellite foci remaining or no significant decline in tumor size. Our combined model serves to predict tumor regression at baseline, offers surgical options to surgeons and patients, and provides guidance on the early modification of therapeutic treatment.

To the best of our knowledge, our study is the first to predict breast tumor regression patterns using MR radiomics. MR examinations both at baseline and post-NAC are clinical routines in our center; hence, the MRI data were easily accessible, and no invasive procedure was needed in our study. A radiomic signature combining DWI and T2WI features was first established in our study. DWI and T2WI have been used to evaluate the tumor response to chemotherapy [19,25]. One MRI feature from each series was extracted to create the radiomic signature. The AUCs of the radiomic signature in the PC and VC were 0.858 and 0.819, respectively, which are both acceptable and satisfactory. Two clinicopathological factors, including node stage and ER status, were found to be closely related to tumor regression patterns. Therefore, these factors were incorporated into the combined model, and the NRI and IDI illustrated the superiority of the combined model over the radiomic signature and the clinical prediction model. A nomogram was established to predict type 1 regression by incorporating two clinical factors and the radiomic signature. The calibration curve and decision curve demonstrated that the model had a good fit to actual observations and had net clinical benefit.

Consistent with the findings of previous literature [26,27], tumors with later nodal stages and higher ER expression levels are less likely to have type 1 regression. In other words, these patients may not be BCS candidates. Researchers have focused on correlating molecular subtypes with tumor regression types, but no consensus has been reached [28,29]. Among 144 patients recruited in this study, the percentages of type 2 regression in luminal breast cancers, HER2-overexpressing breast cancers and TNBCs were 20.8%, 12.0%, and 8.7%, respectively ($p = 0.254$). HER2-overexpressing breast cancers and TNBCs had a lower rate of type 2 regression, which

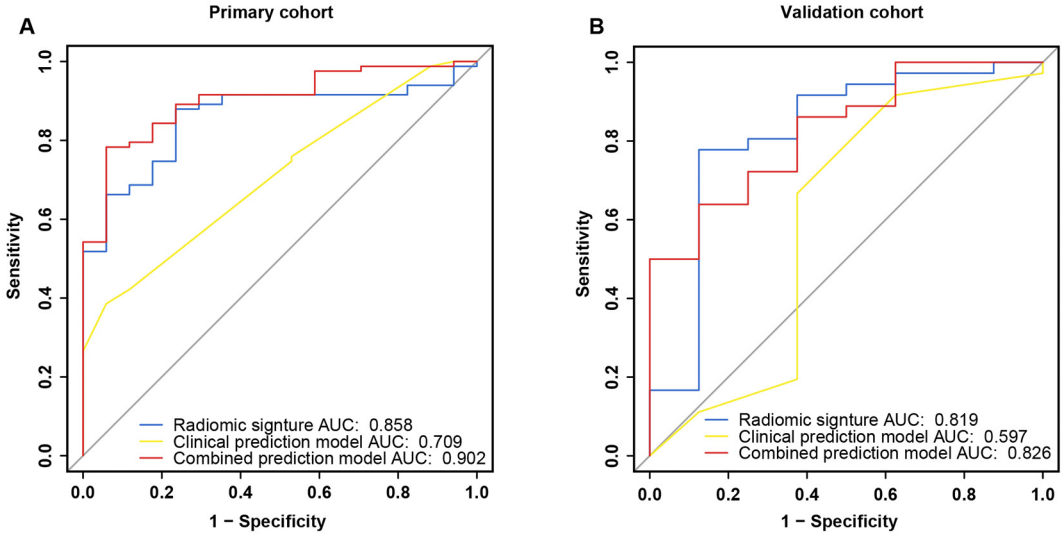

Fig. 3. ROC curves of radiomic signature, clinical prediction model and combined prediction model in both cohorts. a ROC curves in the primary cohort. b ROC curves in the validation cohort.

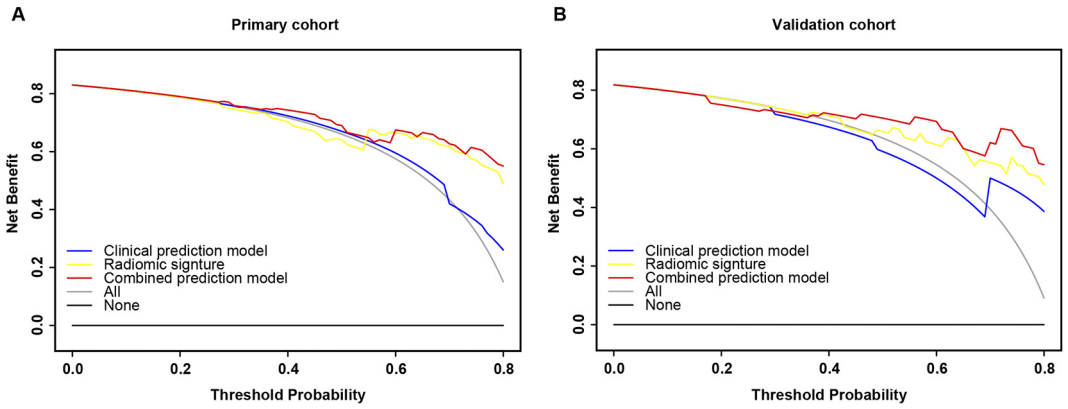

Fig. 4. Decision curve analysis for radiomic signature, clinical prediction model and combined prediction model in both cohorts. The blue line represents the clinical prediction model. The yellow line represents the radiomic signature. The red line represents the combined prediction model. The gray line represents the assumption that all the patients appeared Type 1 tumor regression. The black line represents the assumption that no patients appeared Type 1 tumor regression. a Decision curve analysis in the primary cohort. b Decision curve analysis in the validation cohort.

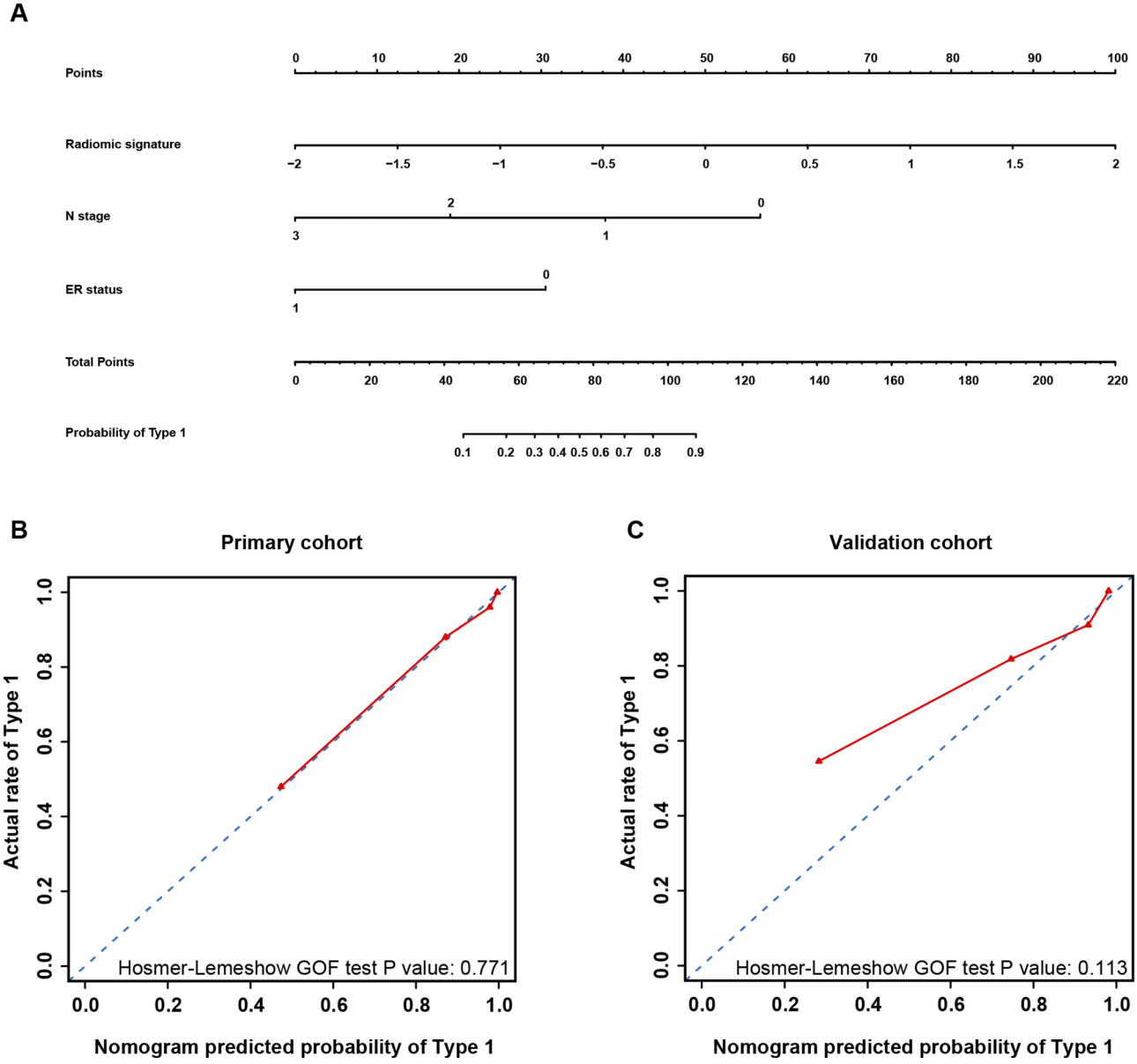

Fig. 5. Nomogram, calibration curve of the nomogram in both cohorts. The red line represents the performance of the nomogram. The blue dotted line represents an ideal prediction. a Nomogram for the combined prediction model. b Calibration curve of the nomogram in the primary cohort. c Calibration curve of the nomogram in the validation cohort.

could be explained by the addition of HER2-targeted therapy in the former and the more invasive nature of the latter.

There are still some limitations in our study. First, the data distribution was imbalanced between the 2 cohorts. Tumors showing type 2 regression are encountered less frequently, which is consistent with clinical observation. Most tumors have good responses to preoperative chemotherapy (and anti-HER2 therapy, e.g., trastuzumab), which leads to pCR or unifocal residual disease after NAC. Second, due to the retrospective nature of our study, only accessible clinical factors could be taken into consideration. The exploration of the correlations between tumor regression and other variables, e.g., a gene signature or an immune signature, is worthwhile. Finally, we did not consider the molecular subtypes separately. The analysis of tumor regression in luminal-type breast cancer would be meaningful.

Conclusions

Our study established a unique model combining a radiomic signature and clinicopathological factors to predict tumor regression patterns prior to the initiation of NAC. The early prediction of type 2 regression offers the opportunity to modify preoperative treatments or aids in determining surgical options.

Declaration of competing interest

The authors declare that they have no known competing financial interests or personal relationships that could have appeared to influence the work reported in this paper.

Acknowledgments

This work was supported by the National Natural Science Foundation of China under Grant Nos. 81871513, 81922040, 81930053, and 81971656; the Beijing Natural Science Foundation under Grant Nos. 7182109 and 7202105; the National Key R&D Program of China under Grant No. 2017YFA0205200; the Youth Innovation Promotion Association CAS under grant number 2019136; the Natural Science Foundation of Guangdong Province, China, under grant number 2017A030313882l; and the CSCO-Constant Rui Tumor Research Fund, China under grant number Y-HR2016-067. The only role of the above funding sources was providing financial support for the conduct of the research.

Ethical approval

All procedures performed in this study, which involved human participants, were in accordance with the ethical standards of the institutional and/or nation research committee and with the 1964 Helsinki Declaration and its later amendments or comparable ethical standards.

Author contribution statement

Xiaosheng Zhuang: Conceptualization; Data curation; Formal analysis; Investigation; Methodology; Software; Writing – original draft; Writing – review & editing.

Chi Chen: Conceptualization; Formal analysis; Investigation; Methodology; Software; Writing – original draft; Writing – review & editing.

Zhenyu Liu: Conceptualization; Formal analysis; Investigation; Methodology;

Liulu Zhang: Data curation; Investigation; Writing – review & editing.

Xuezhi Zhou: Formal analysis; Investigation; Methodology;

Minyi Cheng: Data curation; Writing – original draft.

Fei Ji: Data curation; Writing – original draft.

Teng Zhu: Data curation; Writing – review & editing.

Chuqian Lei: Data curation; Software; Investigation;

Junsheng Zhang: Data curation; Investigation;

Jingying Jiang: Formal analysis; Funding acquisition; Methodology; Resources; Supervision;

Jie Tian: Conceptualization; Funding acquisition; Methodology; Resources; Supervision;

Kun Wang: Conceptualization; Funding acquisition; Resources; Supervision;

References

[1] M. Kaufmann, G.N. Hortobagyi, A. Goldhirsch, S. Scholl, A. Makris, P. Valagussa, et al., Recommendations from an international expert panel on the use of neoadjuvant (primary) systemic treatment of operable breast cancer: an update, J. Clin. Oncol. 24 (12) (2006) 1940–1949.

[2] M.G. Derks, C.J. van de Velde, Neoadjuvant chemotherapy in breast cancer: more than just downsizing, The Lancet Oncology 19 (1) (2018) 2–3.

[3] A. Thompson, S. Moulder-Thompson, Neoadjuvant treatment of breast cancer, Annals of Oncology 23 (suppl_10) (2012) x231-x6.

[4] J. Mieog, J. Van der Hage, C. Van De Velde, Neoadjuvant chemotherapy for operable breast cancer, British Journal of Surgery: Incorporating European Journal of Surgery and Swiss Surgery 94 (10) (2007) 1189–1200.

[5] B. Goorts, K.M. Dreuning, J.B. Houwers, L.F. Kooreman, E.-J.G. Boerma, R.M. Mann, et al., MRI-based response patterns during neoadjuvant chemotherapy can predict pathological (complete) response in patients with breast cancer, Breast Cancer Res. 20 (1) (2018) 34.

[6] D.C. Ling, P.A. Sutera, N.A. Iarrobino, E.J. Diego, A. Soran, R.R. Johnson, et al., Is multifocal regression a risk factor for ipsilateral breast tumor recurrence in the modern era after neoadjuvant chemotherapy and breast conservation therapy? International Journal of Radiation Oncology* Biology* Physics 104 (4) (2019) 869–876.

[7] M.E. Straver, C.E. Loo, E.J. Rutgers, H.S. Oldenburg, J. Wesseling, M.-J.T.V. Peeters, et al., MRI-model to guide the surgical treatment in breast cancer patients after neoadjuvant chemotherapy, Ann. Surg. 251 (4) (2010) 701–707.

[8] I. Fukada, K. Araki, K. Kobayashi, T. Shibayama, S. Takahashi, N. Gomi, et al., Pattern of tumor shrinkage during neoadjuvant chemotherapy is associated with prognosis in low-grade luminal early breast cancer, Radiology. 286 (1) (2018) 49–57.

[9] B. Asselain, W. Barlow, J. Bartlett, J. Bergh, E. Bergsten-Nordström, J. Bliss, et al., Long-term outcomes for neoadjuvant versus adjuvant chemotherapy in early breast cancer: meta-analysis of individual patient data from ten randomised trials, The Lancet Oncology 19 (1) (2018) 27–39.

[10] S. Nakamura, H. Kenjo, T. Nishio, T. Kazama, O. Doi, K. Suzuki, Efficacy of 3D-MR mammography for breast conserving surgery after neoadjuvant chemotherapy, Breast Cancer 9 (1) (2002) 15–19.

[11] W.J. Gradishar, B.O. Anderson, R. Balassanian, S.L. Blair, H.J. Burstein, A. Cyr, et al., Breast cancer, version 4.2017, NCCN clinical practice guidelines in oncology, J. Natl. Compr. Cancer Netw. 16 (3) (2018) 310–320.

[12] F. Poggio, M. Bruzzone, M. Ceppi, N. Pondé, G. La Valle, L. Del Mastro, et al., Platinum-based neoadjuvant chemotherapy in triple-negative breast cancer: a systematic review and meta-analysis, Ann. Oncol. 29 (7) (2018) 1497–1508.

[13] K. Pinker, J. Chin, A.N. Melsaether, E.A. Morris, L. Moy, Precision medicine and radiogenomics in breast cancer: new approaches toward diagnosis and treatment, Radiology. 287 (3) (2018) 732–747.

[14] Z. Liu, Y. Wang, X. Liu, Y. Du, Z. Tang, K. Wang, et al., Radiomics analysis allows for precise prediction of epilepsy in patients with low-grade gliomas, NeuroImage: Clinical 19 (2018) 271–278.

[15] S. Bickelhaupt, F.B. Laun, J. Tesdorff, W. Lederer, H. Daniel, A. Stieber, et al., Fast and noninvasive characterization of suspicious lesions detected at breast cancer X-ray screening: capability of diffusion-weighted MR imaging with MIPs, Radiology. 278 (3) (2016) 689–697.

[16] Y.Q. Huang, C.H. Liang, L. He, J. Tian, C.S. Liang, X. Chen, et al., Development and validation of a Radiomics Nomogram for preoperative prediction of lymph node metastasis in colorectal cancer, J. Clin. Oncol. 34 (18) (2016) 2157–2164.

[17] Z. Liu, X.-Y. Zhang, Y.-J. Shi, L. Wang, H.-T. Zhu, Z. Tang, et al., Radiomics analysis for evaluation of pathological complete response to neoadjuvant chemoradiotherapy in locally advanced rectal cancer, Clin. Cancer Res. 23 (23) (2017) 7253–7262.

[18] N.M. B, M. E, P. P, C. D, H. G, P. T, et al., Erratum to: intratumoral and peritumoral radiomics for the pretreatment prediction of pathological complete response to neoadjuvant chemotherapy based on breast DCE-MRI, Breast cancer research: BCR 19 (1) (2017) 80.

[19] Z. Liu, Z. Li, J. Qu, R. Zhang, X. Zhou, L. Li, et al., Radiomics of multiparametric MRI for pretreatment prediction of pathologic complete response to neoadjuvant chemotherapy in breast cancer: a multicenter study, Clin. Cancer Res. 25 (12) (2019) 3538–3547.

[20] Q. Xiong, X. Zhou, Z. Liu, C. Lei, C. Yang, M. Yang, et al., Multiparametric MRI-based radiomics analysis for prediction of breast cancers insensitive to neoadjuvant chemotherapy, Clin. Transl. Oncol. 22 (1) (2020) 50–59.

[21] T. Fujii, T. Kogawa, W. Dong, A.A. Sahin, S. Moulder, J.K. Litton, et al., Revisiting the definition of estrogen receptor positivity in HER2-negative primary breast cancer, Ann. Oncol. 28 (10) (2017) 2420–2428.

[22] M.C. Cheang, S.K. Chia, D. Voduc, D. Gao, S. Leung, J. Snider, et al., Ki67 index, HER2 status, and prognosis of patients with luminal B breast cancer, JNCI: Journal of the National Cancer Institute 101 (10) (2009) 736–750.

[23] A.S. Coates, E.P. Winer, A. Goldhirsch, R.D. Gelber, M. Gnant, M. Piccart-Gebhart, et al., Tailoring therapies—improving the management of early breast cancer: St Gallen international expert consensus on the primary therapy of early breast cancer 2015, Ann. Oncol. 26 (8) (2015) 1533–1546.

[24] E.A. Eisenhauer, P. Therasse, J. Bogaerts, L.H. Schwartz, D. Sargent, R. Ford, et al., New response evaluation criteria in solid tumours: revised RECIST guideline (version 1.1), Eur. J. Cancer 45 (2) (2009) 228–247.
[25] W. Tan, M. Yang, H. Yang, F. Zhou, W. Shen, Predicting the response to neoadjuvant therapy for early-stage breast cancer: tumor-, blood-, and imaging-related biomarkers, Cancer Manag. Res. 10 (2018) 4333.
[26] S. Wang, Y. Zhang, X. Yang, L. Fan, X. Qi, Q. Chen, et al., Shrink pattern of breast cancer after neoadjuvant chemotherapy and its correlation with clinical pathological factors, World Journal of Surgical Oncology 11 (1) (2013) 166.
[27] J. Raphael, S. Gandhi, N. Li, F.-I. Lu, M. Trudeau, The role of quantitative estrogen receptor status in predicting tumor response at surgery in breast cancer patients treated with neoadjuvant chemotherapy, Breast Cancer Res. Treat. 164 (2) (2017) 285–294.
[28] M. Li, B. Xu, Y. Shao, H. Liu, B. Du, J. Yuan, Magnetic resonance imaging patterns of tumor regression in breast cancer patients after neo-adjuvant chemotherapy, and an analysis of the influencing factors, Breast J. 23 (6) (2017) 656–662.
[29] C.E. Loo, M.E. Straver, S. Rodenhuis, S.H. Muller, J. Wesseling, M.-J.T. Vrancken Peeters, et al., Magnetic resonance imaging response monitoring of breast cancer during neoadjuvant chemotherapy: relevance of breast cancer subtype, J. Clin. Oncol. 29 (6) (2011) 660–666.